

Entanglement transition of elastic lines in a strongly disordered environment

VILJO PETÄJÄ¹, MIKKO ALAVA^{1,2} and HEIKO RIEGER³

¹ *Helsinki University of Techn., Lab. of Physics, P.O.Box 1100, 02015 HUT, Finland*

² *SMC-INFM, Dipartimento di Fisica, Università “La Sapienza”, P.le A. Moro 2 00185 Roma, Italy*

³ *Theoretische Physik, Universität des Saarlandes, 66041 Saarbrücken, Germany*

PACS. 05.40.-a – Fluctuation phenomena etc..

PACS. 74.25.Qt – Vortex lattices, flux pinning, flux creep.

PACS. 74.62.Dh – Effects of crystal defects, doping etc..

Abstract. – We investigate by exact optimization the geometrical properties of three-dimensional elastic line systems with point disorder and hard-core repulsion. The line ‘forests’ become *entangled* due to increasing line wandering as the system height is increased, at fixed line density. There is a transition height at which a cluster of pairwise entangled lines spans the system, transverse to average line orientation. Numerical evidence implies that the phenomenon is in the ordinary percolation universality class. Similar results are obtained for an ensemble of flux lines obeying random walk -dynamics.

The topological entanglement of line-like elastic objects is an important physical phenomenon for a number of interacting many-body systems. Examples are the entanglement of magnetic flux lines in high- T_c superconductors in the mixed phase [1, 2] or of polymers in materials like rubber [3]. The degree of entanglement usually manifests itself in various measurable properties like stiffness or shear modulus in the case of polymers and in transport or dynamical properties for magnetic flux lines in superconductors.

In the latter case the entanglement is caused either by thermal fluctuations [1, 4] or sufficiently strong quenched disorder through lattice defects or pinning centers [5, 6, 11] and varies with the line density, i.e. the strength of the applied magnetic field. A strongly disordered high- T_c superconductor is in a vortex glass state [7], which is superconducting (or has at least an extremely small resistivity) and in which the Abrikosov flux line lattice is destroyed as in the non-superconducting vortex liquid state. At weaker disorder or at smaller magnetic fields a transition to a Bragg glass phase [8], in which the positions of the flux lines show quasi-long-range order, takes place. This has been observed experimentally [9] and in simulations [10]. In contrast to this (quasi)-ordered solid, the lines in the vortex glass phase are expected to be strongly entangled [12]. Since the vortex glass proposed in [7] corresponds to glassy order in the phase of the superconducting order parameter it is not a priori clear that an entangled phase corresponds to this, it could be another type of glassy phase, or smoothly connected to a liquid. In any case an entangled phase will be different from the Bragg glass phase, and an

elastic description, the usual theoretical starting point [8], is inappropriate due to the drastic increase in the transverse line fluctuations. An understanding of such topologically highly non-trivial states including the conditions under which it occurs is highly desirable.

Here we study a model for an ensemble of elastic lines exposed to strong point disorder and focus on the transition from independent lines to entangled bundles of lines. Due to the disorder potential the lines make transverse excursions even at zero temperature, and wind around each other. We introduce a computationally convenient measure for the entanglement of two lines via their winding angle and study clusters of mutually entangled lines. The physical properties of the line system are expected to change drastically (if compared with an unentangled, Bragg-glass like case) with the size of these clusters. Beyond a particular height of the system, dependent on the line density ρ , a percolating bundle of entangled lines is formed. It spans the transverse system size — representing a disorder induced braided flux phase. Thus, in accordance with an observation by Nelson for the thermal case [1], in sufficiently thin samples the lines behave like disentangled rods (still pinned by the disorder), whereas for thick enough systems there is an entanglement transition. This takes place also if the line density is varied - in high- T_c superconductors - by the magnetic field, though our model is strictly appropriate at relatively low densities when the line-line interactions are weak. This transition may be visible in experiments [9] with a Bragg glass phase and a vortex glass phase, in which flux lines are expected to be entangled (although experimentally line entanglement might be difficult to measure). The results are contrasted with a simulation of a (2+1)-dimensional set of random walkers - mimicking thermally fluctuating flux lines with hard core repulsion - with a similar entanglement transition.

The three-dimensional disordered environment has lines living on the bonds of a simple cubic lattice with a lateral width L and a longitudinal height h ($L \times L \times h$ sites) with free boundary conditions in all directions. Each line starts and ends at an arbitrary position on the bottom respective top planes. The number N of lines is fixed by a prescribed density $\rho = N/L^2$. The lines have hard-core interactions: the configuration is specified by bond-variables $n_i = 1$, indicating a line segment occupying bond i , and $n_i = 0$ for vacant bonds. Note that we allow line crossing at the lattice sites, and thus the line identification based upon a bond configuration is not unique.

We model the disordered environment by assigning a random (potential) energy $e_i \in [0, 1]$ (uniformly distributed) to each bond i . The total energy of a configuration is given by

$$H = \sum_i e_i n_i . \quad (1)$$

An elastic energy term is intrinsically present in this model (i.e. is generated upon coarse graining [13]) since the positivity of the energies e_i disfavor in general large transverse excursions of the lines. An equivalent continuum version is

$$\mathcal{H} = \sum_{i=1}^N \int_0^h dz \left\{ \frac{\gamma}{2} \left[\frac{d\mathbf{r}_i}{dz} \right]^2 + \sum_{j(\neq i)} V_{\text{int}}[\mathbf{r}_i(z) - \mathbf{r}_j(z)] + V_r[\mathbf{r}_i(z), z] \right\} . \quad (2)$$

where $\mathbf{r}_i(z)$ denotes the transversal coordinate at longitudinal height z of the i -th flux line and where, in order to version (1) the interactions $V_{\text{int}}[\mathbf{r}_i(z) - \mathbf{r}_j(z)]$ have to be short ranged (i.e. in case of flux lines the screening length small compared to the average line distance) or just hard core repulsive, and the random, δ -correlated disorder potential $V_r[\mathbf{r}_i(z), z]$ has to be strong compared to the elastic energy ($\propto \gamma$).

At low temperatures the line configurations will be dominated by the disorder and thermal fluctuations are negligible. We focus ourselves to zero temperature, the ground state of

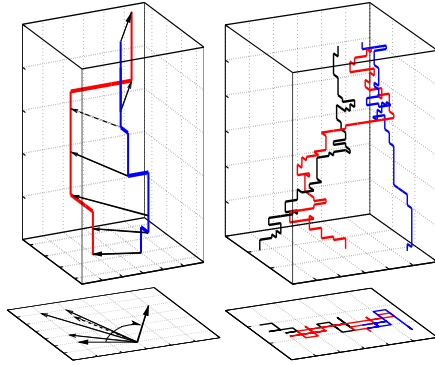


Fig. 1 – Left: Definition of the winding angle of two flux lines: For each z -coordinate the vector connecting the two lines is projected onto that basal plane. $z = 0$ gives the reference line with respect to which the consecutive vectors for increasing z -coordinate have an angle $\phi(z)$. Once $\phi(z) > 2\pi$ the two lines are said to be entangled. Right, top: A configuration of three lines that are entangled. Right, bottom: The projection of the line configuration on the basal plane, defining a connected cluster.

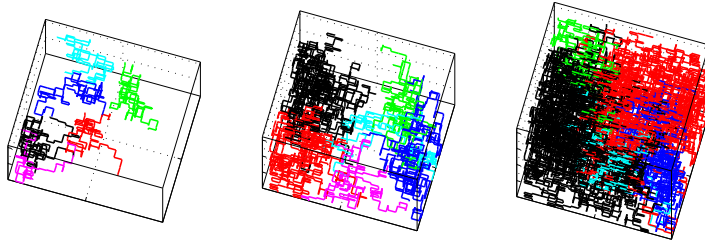


Fig. 2 – Line configurations for different heights h (from left to right: $h = 64, 96, 128$), the lateral size $L = 20$, the line density is $\rho = 0.3$. Only the largest line bundles are shown, indicated by a varying grey scale. Black denotes the largest cluster, which eventually percolates.

the energy (1). The computation thereof is a non-trivial task and is done by applying the polynomial Dijkstra's shortest path algorithm, successively on a residual graph [13, 14].

The line configuration is then analyzed by computing the winding angle of all line pairs as indicated in Fig. 1 (c.f. [15]). We define two lines to be *entangled* when this winding angle becomes larger than 2π . This measures entanglement from the topological perspective [12], arising from the requirement that an entangled pair of lines can not be separated by a linear transformation in the basal plane (i.e. the lines almost always would cut each other, if one were shifted). The precise definition of entanglement is not of major relevance, this being the computationally easiest.

Sets or *bundles* of pairwise entangled lines are formed so that a line belongs to a bundle if it is entangled at least with one other line in the set. Such bundles are spaghetti-like — i.e. topologically complicated and knotted sets of one-dimensional objects. Their size distribution is found by a projection on the basal plane, (Fig. 1), a bundle projecting onto a connected cluster. The probability for two-line entanglement increases with system height. Consequently the bundles and their projections (clusters) grow with h , as exemplified in Fig. 2. For the largest height the largest cluster spans from one side of the system to the other, i.e. it *percolates*. Hence, for a given line density ρ we expect that for system heights larger than a finite critical value h_c a spanning entangled bundle occurs, containing an infinite number of lines in the limit $L \rightarrow \infty$. We denote this an *entanglement transition*. In the projection plane this is like a percolation transition, whose properties are investigated next.

The numerical data has been obtained by averaging over up to 10^3 realizations of the random potentials e_i in (1) and the resulting statistical error is in all cases smaller than the symbol size. We studied different line densities between $\rho = 0.1$ and $\rho = 0.5$, but present

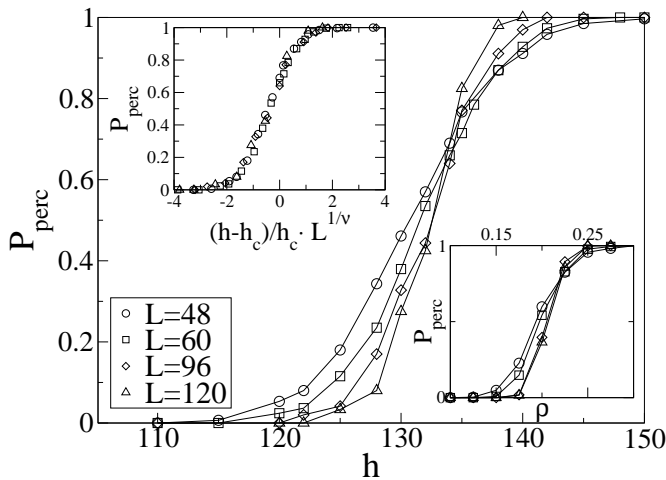


Fig. 3 – Percolation probability for different lateral system sizes L as a function of the system height h , the line density is $\rho = 0.3$. **Upper inset:** Scaling plot of the data with $h_c = 134$ and $\nu = 4/3$. **Lower inset:** Behavior for $h = 150$, with ρ as the control parameter.

for brevity only data for $\rho = 0.3$. The ρ -dependence of the non-universal quantities like h_c is discussed later — the exponents we report are universal.

In Fig. 3 we show the probability P_{perc} of the clusters of entangled bundles, to percolate as a function of the height h of the system. The curves for different lateral system sizes L intersect at h_c , which gives our estimate for $h_c(\rho = 0.3) = 134$. The upper inset shows a scaling plot according to

$$P_{\text{perc}} = p(L^{1/\nu}\delta) \quad (3)$$

with $\delta = (h - h_c)/h_c$ the reduced distance from the critical height and $\nu = 4/3$ the correlation length exponent. The finite size corrections for smaller system sizes than those shown are larger due to single lines percolating. The lower inset demonstrates that the density ρ can also be used as a control parameter. $\nu = 4/3$ is the exponent of conventional bond percolation in two dimensions. Thus we conclude that the transition is in the universality class of conventional 2d percolation. Other quantities confirm this result: Fig. 4 shows the cluster size distribution $P(n)$ at $h = h_c$ for various L and we find it that it approaches

$$P(n) \propto n^{-\tau} \quad \text{with} \quad \tau = 187/91 \approx 2.055 \quad (4)$$

in the limit $L \rightarrow \infty$. The inset shows the mass (i.e. number of entangled lines) of the percolating bundle at h_c , which fits well to

$$M \propto L^{d_f} \quad \text{with} \quad d_f = 91/48 \approx 1.896 \quad (5)$$

Both exponents, the cluster distribution exponent τ and the fractal dimension d_f are identical to conventional bond percolation and the order parameter exponent, $\beta = 5/36$ also fits the data reasonably well.

This result is somewhat surprising, since one could expect the entanglement of two lines to have correlations. These, if long ranged, change the percolation universality class [16]. Why this is not true is seen from the probability for two lines with mass center distance r to be entangled, $P_{\phi > 2\pi}(r)$ (Fig. 5). It decays exponentially with r , implying for two-line-entanglement only short range correlations. It scales with the transverse fluctuations of a

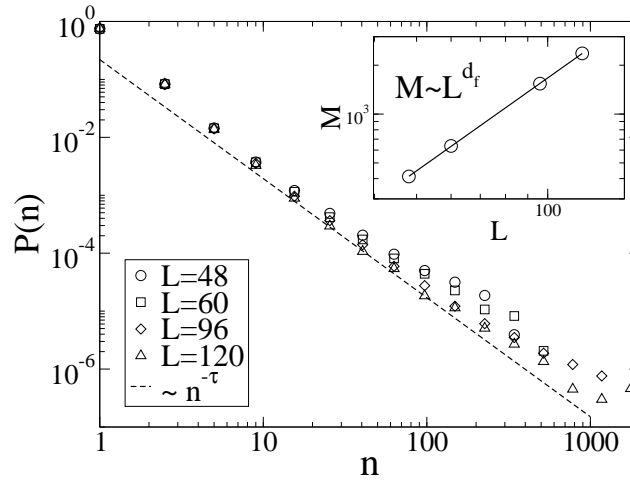


Fig. 4 – Cluster size distributions for different lateral system size at the percolation height $h_c = 134$ in log-log plot. One sees the finite size effects in the tails, the broken line has slope $\tau = 2.06$ and fits the asymptotic ($L \rightarrow \infty$) $P(n) \propto n^{-\tau}$. **Inset:** Log-log-plot of the mass (number of entangled lines) of the percolating cluster at $h_c = 134$ as a function of the lateral size L . The straight line has slope $d_f = 1.90$, the fractal dimension of percolation.

single line h^ζ , where $\zeta = 0.62$ is the single-line roughness exponent in $3d$, [17, 18], so that $P_{\phi > 2\pi}(r) = h^\zeta \tilde{p}(r/h^\zeta)$. It is noteworthy that the “really entangled” lines follow a scaling stemming from single-line behavior. Three-line correlations (e.g. the probability of a third line to be entangled with one or two others, given that these two are entangled or not), are also only short-ranged.

The critical height, h_c , above which an extensive fraction of lines is entangled varies non-

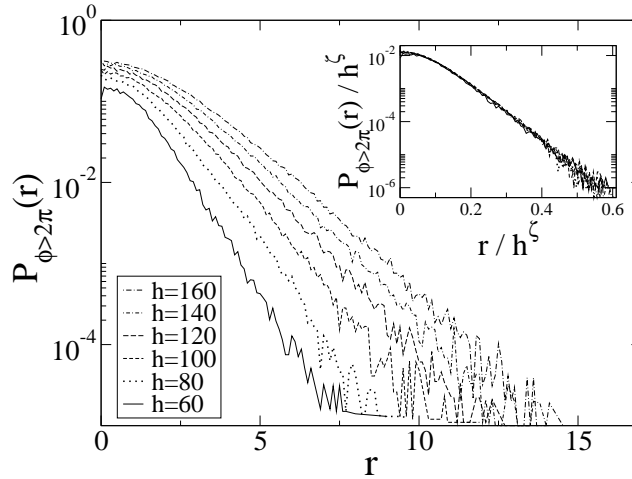


Fig. 5 – Probability $P_{\phi > 2\pi}(r)$ that two lines at a mass center distance r have a winding angle larger than 2π , i.e. are entangled. Inset: Scaling plot, according to $P_{\phi > 2\pi}(r) = h^\zeta \tilde{p}(r/h^\zeta)$. $\zeta = 0.62$ is the single line roughness exponent. The lateral system size is $L = 60$, since $r \ll L$ there is no finite L effect.

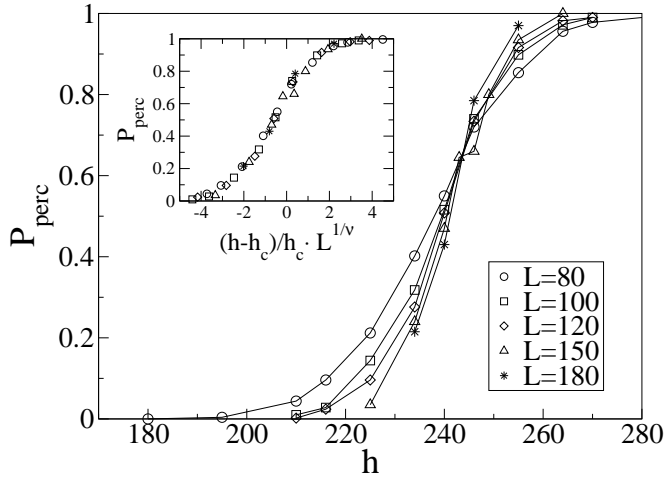


Fig. 6 – Percolation probability for the random walk –case, as a function of the system height h , the line density is $\rho = 0.1$. **Inset:** Scaling plot of the data with $h_c = 244$ and $\nu = 4/3$.

monotonically with the line density ρ . We expect that $h_c \rightarrow \infty$ in both limits $\rho \rightarrow 0$, i.e. very dilute system, and $\rho \rightarrow 1$, very dense systems. In the former case because the line fluctuations $w \propto h^\zeta$ should be of the same order of magnitude as the typical line-to-line distance $d = 1/\sqrt{\rho}$. For this the height has, obviously, to be large enough (see Fig. 3 in which $h = 150$ was chosen to study percolation with ρ). In the opposite limit of a dense system the effective stiffness starts to increase due to the hard core interactions (ie. a lack of vacancies, or unoccupied bonds). Hence $h_c(\rho)$ has a minimum between these two limits, in practice around $\rho = 0.4$. Our estimates for the critical exponents are independent of ρ , but the quality of the data deteriorates due to fewer samples. We expect that for all ρ the entanglement transition is in the percolation universality class.

The previous picture of the development of entanglement underscores the weak correlations in the line ensemble - the character of the ground state enters mostly via single-line roughness exponents. An analogous question can be put forth in the hypothetical case of $N = \rho L^2$ flux lines, that roughen thermally but do not interact except via hard-core expulsion. In this thermal case flux lines are modeled by an configuration of simultaneously evolved non-overlapping random walks on the tilted cubic lattice where z -direction represents the time. At each step $z \rightarrow z + 1$ all walks in a randomly chosen order make a step using non-occupied bonds. Results are shown in Fig. 6, and can be compared with Fig. 3. The data collapses as before, and does so for $P_{\phi > 2\pi}(r)$ with the single-random walk roughness exponent $(1/2)$.

To conclude we studied the entanglement transition of hard core repulsive lines in a disordered environment, driven by the system thickness or the line density. We find two transitions or a non-monotonic behavior of $h_c(\rho)$, for sufficiently thick samples. The one at low densities may be, in the presence of strong point disorder, located close to the the Bragg to vortex glass transition [9,10]. A signature of this would be a dependence of the order-disorder phase boundary on the sample thickness. Above the transition an extensive line bundle is formed. It presents a topological obstacle for also those lines that are not part of it, due to the energy cost of vortex-vortex cutting. In the proximity of the transition there is a wide variety of bundle sizes, in full analogy with usual percolation. This has implications for *bundle depinning*, a collective effect that depends on the bundle size [19], if an external current is applied, and thus on vortex flow both for bundles and single vortices. In analogy with thermal entanglement [1]

one expects also the critical current to increase [20].

It would be interesting to study the modifications of the entanglement transition due to splayed line defects [6], or other forms of correlated disorder. Moreover, it would be highly desirable to include long-range interactions among the lines, since only in their presence a Bragg glass phase on the low disorder or low line density side will occur. The addition of thermal fluctuations, neglected here, will lead to another interesting transition, from an entangled vortex glass to an entangled vortex liquid.

* * *

The support of the European Science foundation (ESF) SPHINX network, the Deutsche Forschungsgemeinschaft (DFG), and (MJA, VIP) the Center of Excellence program of the Academy of Finland is acknowledged.

REFERENCES

- [1] D. R. Nelson, Phys. Rev. Lett. **60**, 1973 (1988); D. R. Nelson and S. Seung, Phys. Rev. B **39**, 9153 (1989).
- [2] For a review see G. Blatter et al., Rev. Mod. Phys. **66**, 1125 (1994).
- [3] M. Doi and S. F. Edwards, *The theory of Polymer Dynamics*, (Oxford University Press, Oxford, 1986).
- [4] Y.-H. Li and S. Teitel, Phys. Rev. B **49**, 4136 (1994); A. K. Nguyen, A. Sudbo, and R. E. Hetzel, Phys. Rev. Lett. **77**, 1592 (1996); H. Nordborg and G. Blatter, Phys. Rev. Lett. **79**, 1925 (1997) and Phys. Rev. B **58**, 14556 (1998); Y. Nonomura, X. Hu, and M. Tachiki, Phys. Rev. B **59**, R11657 (1999).
- [5] S. P. Obukhov and M. Rubinstein, Phys. Rev. Lett. **65**, 1279 (1990).
- [6] T. Hwa, P. Le Doussal, D. R. Nelson, and V. M. Vinokur, Phys. Rev. Lett. **71**, 3545 (1993).
- [7] M. P. A. Fisher, Phys. Rev. Lett. **62**, 1415 (1989); D. S. Fisher et al, Phys. Rev. B **43**, 130 (1991).
- [8] T. Nattermann, Phys. Rev. Lett. **64**, 2454 (1990); T. Giarmachi and P. Le Doussal, Phys. Rev. Lett. **72**, 1530 (1994); and Phys. Rev. B **52**, 1242 (1995).
- [9] B. Khaykovich et al., Phys. Rev. Lett. **76**, 2555 (1996); K. Deligiannis et al., Phys. Rev. Lett. **79**, 2121 (1997); I. Jourmard et al., Phys. Rev. Lett. **82**, 4930 (1999); Y. Paltiel et al., Phys. Rev. Lett. **85**, 3712 (2000).
- [10] Y. Nonomura and X. Hu, Phys. Rev. Lett. **85**, 5140 (2001).
- [11] D. López et al., Phys. Rev. Lett. **80**, 1070 (1998); L. M. Paulius et al., Phys. Rev. B **61**, R11910 (2000).
- [12] K. V. Samokhin, Phys. Rev. Lett. **84**, 1304 (2000); R. Bikbov and S. Nechaev, Phys. Rev. Lett. **87**, 150602 (2001).
- [13] M. Alava, P. Duxbury, C. Moukarzel, and H. Rieger: *Combinatorial optimization and disordered systems*, “Phase Transitions and Critical Phenomena”, vol. 18., (ed. C. Domb and J. L. Lebowitz) (Academic Press, 2000); A. Hartmann and H. Rieger, *Optimization Algorithms in Physics*, (Wiley VCH, Berlin, 2002).
- [14] H. Rieger, Phys. Rev. Lett. **81**, 4488 (1998).
- [15] B. Drossel and M. Kardar, Phys. Rev. E **53**, 5861 (1996).
- [16] A. Weinrib, Phys. Rev. B **29**, 387 (1984).
- [17] T. Halpin-Healy and Y.-C. Zhang, Physics Reports **254**, 215 (1995).
- [18] J. M. Kim, M. A. Moore and A. J. Bray, Phys. Rev. A **44**, 2345 (1991); N. Schwartz, A. L. Nazaryev and S. Havlin, Phys. Rev. E **58**, 7642 (1998); E. Perlsman and S. Havlin, Phys. Rev. E **63**, 010102 (2001).
- [19] W. J. Yeh and Y. H. Kao, Phys. Rev. B **44**, 360 (1991)
- [20] C. J. van der Beek et al., Phys. Rev. B **66**, 024523 (2002)